THE UPC SCANNING RAMAN LIDAR: AN ENGINEERING OVERVIEW

Francesc Rocadenbosch[a], Michaël Sicard[b], Adolfo Comerón[a], José María Baldasano[c], Alejandro Rodríguez[a], Ravil Agishev[a], Constantino Muñoz[a], Miguel Ángel López[a], David García-Vizcaíno[a]

[a]Universitat Politècnica de Catalunya (UPC), Dep. of Signal Theory and Communications
[b]Service d'Aéronomie, Institut Pierre-Simon-Laplace, Université Pierre et Marie Curie, Paris
[c]Universitat Politècnica de Catalunya (UPC), Dep. of Engineering Projects

INTRODUCTION

- Active remote sensing with LIDAR (LIght Detection And Ranging), as compared to passive systems and active sensing with microwave radars, offers much better spatial resolutions (on the order of a few meters) and optical wavelengths often comparable to the size of the target aerosols so that the backscattered return radiation conveys prime range-resolved information about the intervening atmosphere.
- Lidar observations at mesoscale and local scales are of prime importance for pollution monitoring and environmental modelling for aerosols play an important role in many atmospheric topics (e.g. Earth-atmosphere radiative budget, cloud formation, pollution transport and atmospheric photochemistry).
- An innovative approach to overcome the lack of quantitative information (mainly, mass concentration, extinction and backscatter profiles and, quite often temperature and humidity profiles as well) is to combine at least one elastic (i.e. no wavelength shift in the return radiation) with one inelastic (i.e. Raman shifted) receiving channel. The UPC lidar system combines 2+1 elastic/Raman channels plus a scanning feature into a single portable 3-D-*scanning Raman lidar* (SRL) instrument.

SCANNING RAMAN LIDAR (SRL) SYSTEM ARCHITECTURE OVERVIEW

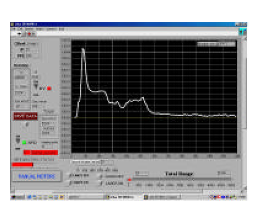

Full system control from LabView™.

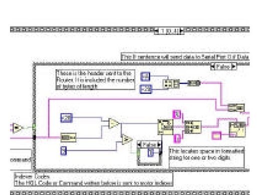

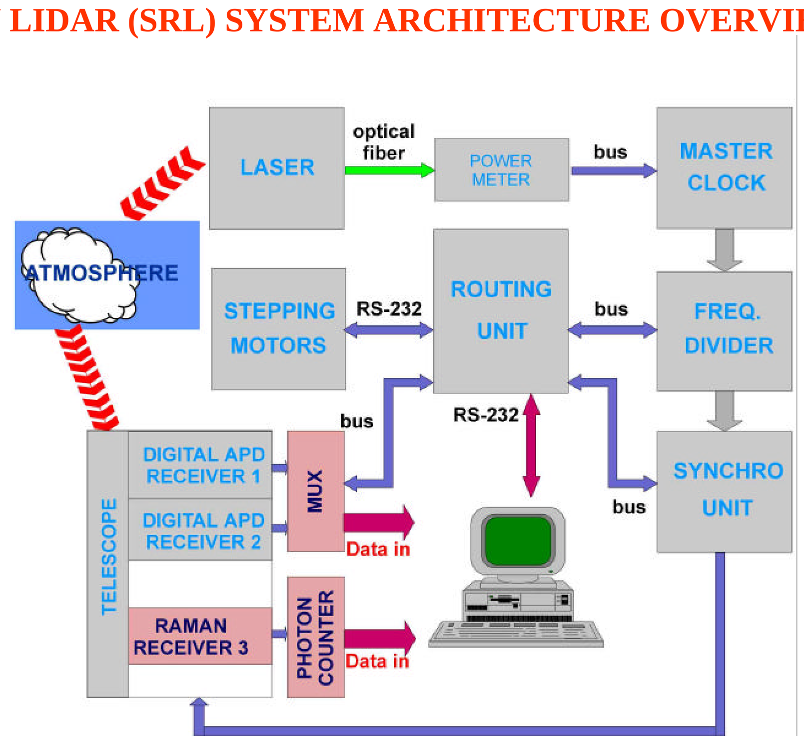

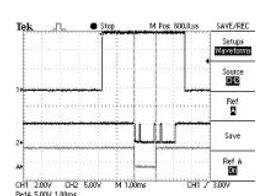

The routing unit passes control data bursts on to its slave devices.

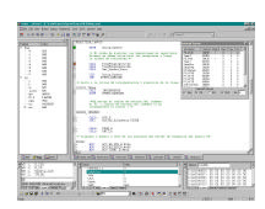

MOTIVATION FOR THE DOUBLE-WINDOW APPROACH

Effective noise quantization is essential to benefit from integration gain:

(a) Range-corrected lidar signal (scene1).

(b) Raw-voltage record counterpart at the ADC (analog-to-digital converter) output in the 8-10-km-range interval. Bad noise quantization (500 pulses averaged) shows up as noise spikes.

(c)(d) Same as (a)(b) for scene 2. In (d), proper gain and offset adjustment in the far-range window (13-15 km) yields to very good noise quantization so that the nominal integration gain is reached.

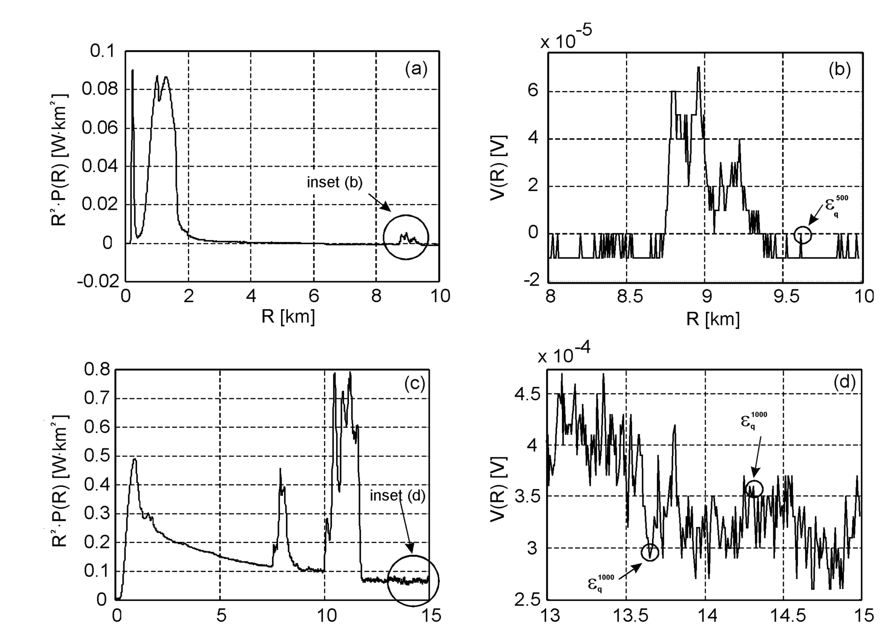

THE DOUBLE-WINDOW TECHNIQUE

By using dual window exploration, the equivalent dynamic range of the elastic lidar channels can largely be expanded.

Thus, instead of fitting the full lidar exploration range (A'-D') into the dynamic range of the ADC, a partitioned approach is used to accommodate range A-B into the ADC at the odd pulses while range C-D at the even ones. At each succeeding shot, the elastic receivers are gated so that the control system (routing unit) ping-pongs new gain and offset receiver settings accordingly.

As a result, the lidar is able to perform interspersed short-range [$R_{min,1}$, $R_{max,1}$] (AB window) and far-range [$R_{min,2}$, $R_{max,2}$] (CD window) exploration, hence benefiting of enhanced dynamic range.

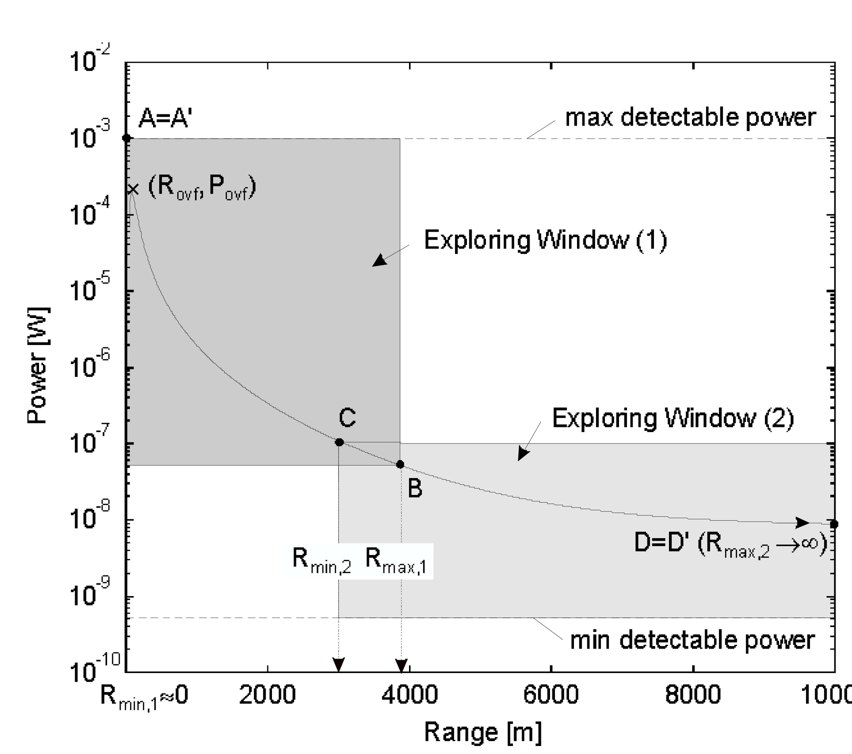

OPTO-MECHANICAL OVERVIEW

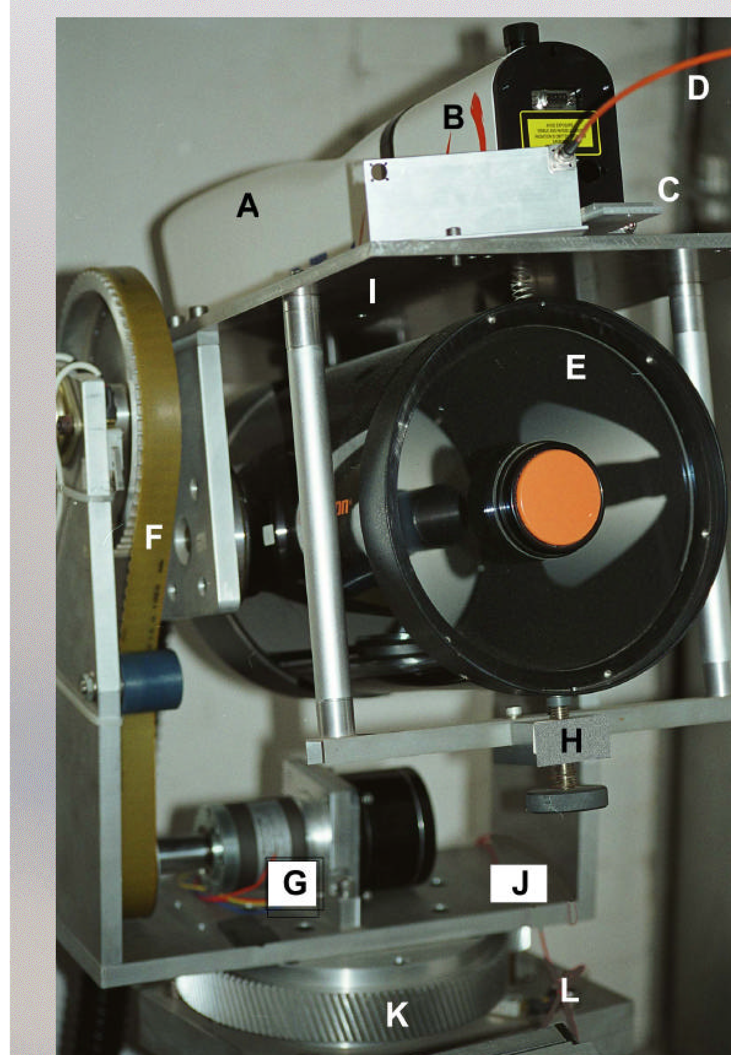

Front view of the portable *Scanning Raman Lidar (SRL):*

A. Nd:YAG laser
B. Frequency doubler
C. Polariser assembly
D. Master clock fiber
E. Receiving telescope
F. Elevation gears and reduction belt
G. Elevation stepping motor and on-axis reductor
H. Elevation screw for overlap factor adjustment
I. Laser platform
J. U-fork
K. Azimuth reduction gear
L. Emergency stop switches

SYSTEM SPECIFICATIONS

Scanning capabilities		Scanning range	120º × 300º
		Angular precision	2 arc. min.
EMITTER	Laser	Mod.	Quantel Brillant 20
		Output (using frequency doubler)	Nd:YAG 532/1064 nm
			2×160 mJ / 0.5 mrad
		Pulse specs	5-10 ns / 20 Hz
	Polariser	Mod.	Newport PR-950
		Bandwidth	700-1200 nm
RECEIVER	Telescope	Type	Schmidt-Cassegrain
		Diameter	20 cm
		Focal length	2 m
		FOV	0.75 mrad ≈ 2.6 arc. min.
Elastic channels:		Wavelengths	532 nm, 1064 nm
		Spectral bandwidth	10 nm
		Min. Det. Power (S/N = 1)	1.6 nW (single pulse)
		NEP (APD receivers)	1.5×10^{-13} W·Hz$^{-1/2}$
		Spatial resolution	7.5 m
	APD	Mod.	Perkin Elmer C30956E (532/1064 nm)
		Responsivity	18 A/W (532 nm)
			20 A/W (1064 nm)
		Dark current	120 nA
		Internal gain	150
	PMT	Mod.	Hamamatsu R7400P-06
		Anode radiant sensitivity	4.3×10^{4} A/W (532 nm)
		Anode dark current	0.4 nA (30 ºC) / 80 cps
		Internal gain	10^{6}
	Acquisition card	Mod.	Spectrum MI.3011
			2×20 Msps/12 bit
			SNR > 67 dB (20 MHz)
Raman channel:		Wavelength	607.4 nm (N_2/532 nm)
		Spectral bandwidth	3 nm
		Photon counting limit	0.6 fW
		Min. Det. Power (S/N = 1)	0.5 nW (single pulse)
		NEP (PMT receiver)	9.1×10^{-16} W·Hz$^{-1/2}$
		Spatial resolution	7.5 m
	PMT	Mod.	Hamamatsu R7400P-01
		Anode radiant sensitivity	3×10^{4} A/W (607.4 nm)
		Anode dark current	1 nA (30 ºC) / 500 cps
		Internal gain	10^{6}
	Counter	Mod.	Licel TR20-160
		Type	Mixed 250-MHz Photon Counter + ADC 20 Msps 12-bit

THREE-CHANNEL RECEIVING FRONT-END LAYOUT OF THE SRL

In an elastic-Raman system, the Raman-shifted radiation backscattered by N_2-molecules in the atmosphere (of known proportion) is used as a self-calibration signal for the elastic channels. As a result, reliable independent measurement of the particle atmospheric extinction, backscatter and lidar ratio profiles is possible. In order to do that, the optical receiver front-end separates the three receiving wavelengths as shown:

(A) 1.5-mm-diameter fiber conveying the 3 receiving wavelengths
(B) Fiber optics collimator
(C)(D) Dichroic beam splitters
(E) 607.4-nm PMT-based receiver (output to the photon counter)
(F)(G) 532-nm and 1064-nm APD-based receivers featuring digital remote control and dual-window operation (output to ADC)
(H) Coupling cylinders housing focusing lens + IF filter

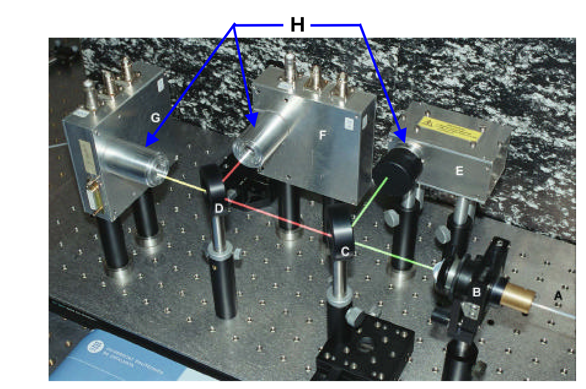

LINK BUDGET: RECEIVED POWER AND SIGNAL-TO-NOISE RATIO

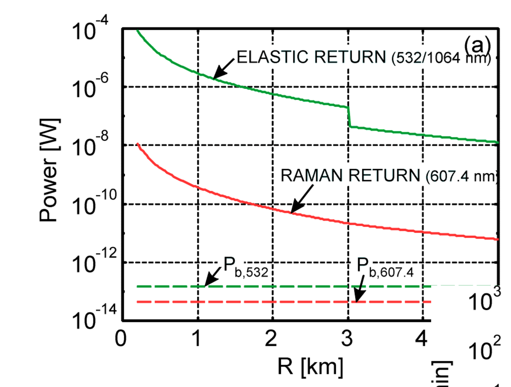

(a) Elastic and Raman return power signals (single pulse) vs. range. Horizontal lines indicate background levels.

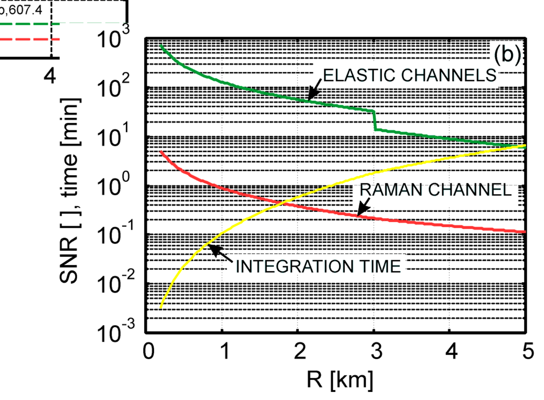

(b) SNR vs. range along with the integration time to reach a 20-dB goal (S/N=10) in the Raman channel (analog mode).

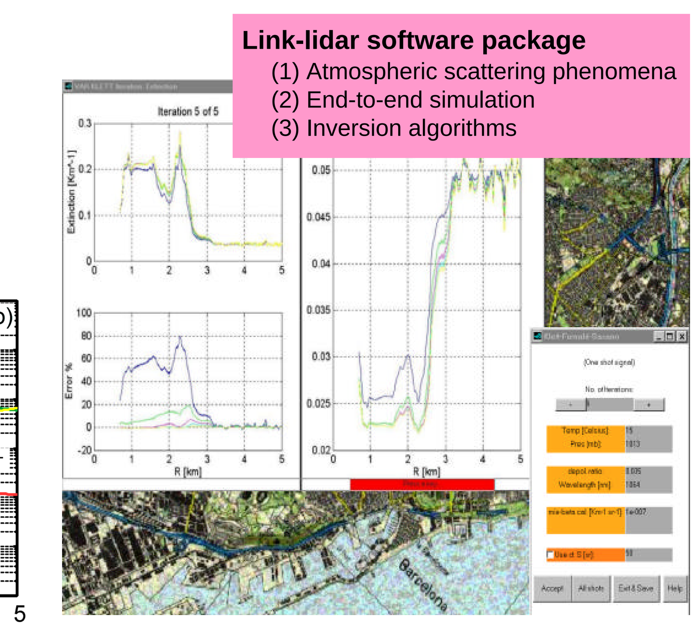

Data were simulated for a homogeneous atmosphere (visibility V_M=39.12 km, extinction coefficient α=0.1 km^{-1}, lidar ratio S=25sr^{-1}) up to a boundary layer height of 3.0 km. A U.S. standard atmosphere with a ground pressure of 1013 hPa and a ground temperature of 15ºC up to a tropopause height of 12 km was assumed. An incomplete overlap of laser beam and receiver field of view below 200 m was introduced. Full-moon background radiance (night-time operation), signal-shot noise, dark-current shot noise, thermal noise and typical system parameters from the specs. table (center poster) were considered as well.

MEASUREMENT EXAMPLE

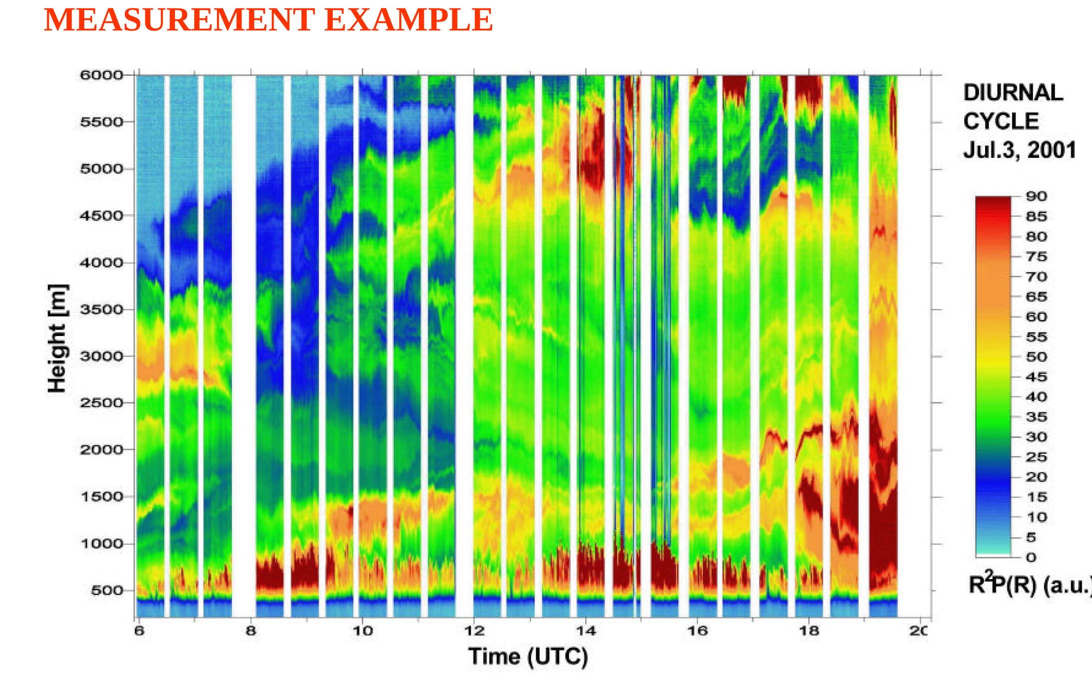

The graph illustrates PBL formation from 6:00 UTC until 10:00. Analytical backtrajectory cross-analyses indicate a recirculation situation, with air masses having moved very little in the four previous days and, up to 500 hPa, mainly over France and the Iberian peninsula (e.g. thicker layer after 18:00 raised by its passage over the Pyrenees). Day conditions: Extremely low baric gradient with very weak winds, sunny with occasional broken clouds above 6000 m (after lidar data).

CONCLUSIONS

An interesting step towards the derivation of independent extinction and backscatter profiles is the set-up of cooperative multiwavelength channels into an elastic-Raman lidar. Besides, when a scanning feature is added to build a 3-D SRL, wind vector measurements are also possible by using airborne aerosols as tracers. As a result, a volume imaging lidar can be implemented. System engineering is aimed at fostering portability in terms of modular desing and scalability.

The Scanning Raman Lidar system is currently being operated by the EEF lidar group at UPC within the EARLINET european network, which is composed of over 21 ground-based lidars, on a regular basis.

ACKNOWLEDGEMENTS

The author wishes to acknowledge the following entities for partially supporting the research work and lidar systems developed at UPC: European Union under the EARLINET contract UE EVR1-CT-1999-40003, CICYT (Spanish Interministry Comission of Science and Technology) under the grants TIC 431/93, AMB96-1144-C02-C01, TIC99-1050-C03-01, REN2000-1907-CE and REN2000-1754-C02-02/CLI, Spanish Ministry for Education and Culture under the Spanish-French Integrated Action HF1997-0212, and CIRIT (Interdepartmental Commission for Research and Technological Innovation, Generalitat de Catalunya) under the contract IMMPACTE. ESA is also thanked for the external postdoctoral fellowship allocated to M. Sicard.

Corresponding author: Francesc Rocadenbosch, Universitat Politècnica de Catalunya (UPC), Dep. of Signal Theory and Communications, Group of Electromagnetic Engineering and Photonics (EEF), C/Jordi Girona 1-3, D4-016, 08034 Barcelona, Spain; Email: roca@tsc.upc.es; Phone: +34-93-401-60-85; Fax: +34-93-401-72-32; http//www-tsc.upc.es/eef